

treated with bevacizumab and finished the 24 weeks follow-up. A total of 165 eyes (52.2%) finished the 48 weeks follow-up. We are aware that at 48 weeks, there is significant loss of patients from follow-up, but with 165 eyes, the number is still large. More importantly, between 24 and 48 weeks, there is stabilization of the median VA, the median CRT, the percentage of eyes with a gain of at least three VA lines and the percentage of eyes with no residual ME (Epstein et al. 2012) indicating reliable results also at 48 weeks. At 24 weeks, 44.6% (141 eyes) gained at least three lines (mean of 2.7 injections), and at 48 weeks 48.5% (80 eyes, mean of 4.7 injections). Optical coherence tomography (OCT) examination was performed in 81% (256 eyes) at week 24. Of those, 46% (118 eyes) showed no residual ME with a CRT below 300 μm . Optical coherence tomography (OCT) examination was performed in 128 eyes at 48 weeks, of those, 45% (58 eyes) revealed no residual ME defined as a CRT of <300 μm .

We found a significant impact of the number of injections applied on the improvement of BCVA at 12 and 24 weeks (ANOVA $p = 0.007$ and $p = 0.048$, respectively): In the first 12 weeks, two injections were needed to achieve a median gain of three lines, at 24 weeks, a minimum of three injections was needed to achieve a median improvement of three lines. At 48 weeks, five or less injections revealed a median gain of two BCVA lines, whereas 6 and more injections resulted in a median gain of three BCVA lines. However, the latter was not statistically significant ($p > 0.25$) which may be explained by the low number of eyes enclosed in each subgroup. Therefore, our 48 weeks data should be regarded carefully. Whether monthly injections during the first 3 months would have been associated with a gain of more than three VA lines cannot be answered with our data. However, Epstein and colleagues (2012) performed fixed bevacizumab injections every 6 weeks over 12 months and did not find a gain of more than three lines until week 12.

Several randomized controlled trials (RCTs) and three meta-analyses with 5, 6 and 7 relevant RCTs included (Huang et al. 2013; Pielen et al. 2013; Braithwaite et al. 2014) investigated injection schemes with intravitreal anti-vascular endothelial growth factor (VEGF) agents that effectively reduce ME and

increase BCVA in CRVO (level 1b and 1a evidence, respectively). Besides the level 1 treatment efficacy, the minimal number of injections needed to maximize and maintain the therapeutic effect has not been analysed in the literature, yet. Therefore, we found it highly important to look at this in a routine clinical setting.

References

- Braithwaite T, Nanji AA, Lindsley K & Greenberg PB (2014): Anti-vascular endothelial growth factor for macular oedema secondary to central retinal vein occlusion. *Cochrane Database Syst Rev* 5: CD007325.
- Călugăru D & Călugăru M (2015): Injection scheme for intravitreal bevacizumab therapy for macular oedema due to central retinal vein occlusion: results of a multicenter study. *Acta Ophthalmol*. [Epub ahead of print].
- Epstein DL, Algvere PV, von Wendt G, Seregard S & Kvanta A (2012): Benefit from bevacizumab for macular edema in central retinal vein occlusion: twelve-month results of a prospective, randomized study. *Ophthalmology* 119: 2587–2591.
- Huang P, Niu W, Ni Z, Wang R & Sun X (2013): A meta-analysis of anti-vascular endothelial growth factor remedy for macular edema secondary to central retinal vein occlusion. *PLoS One* 8: e82454.
- Januschowski K, Dimopoulos S & Szurman P (2015): Injection scheme for intravitreal bevacizumab therapy for macular oedema due to central retinal vein occlusion: results of a multicenter study. *Acta Ophthalmol* 93: e400–402.
- Pielen A, Feltgen N, Isserstedt C, Callizo J, Junker B & Schmucker C (2013): Efficacy and safety of intravitreal therapy in macular edema due to branch and central retinal vein occlusion: a systematic review. *PLoS One* 8: e78538.

Correspondence:

Gesine B. Szurman
Eye Clinic Sulzbach
Knappschaftsklinikum Saar
An der Klinik 10
D-66280 Sulzbach
Germany
Tel: 06897 575 1119
Fax: 06897 574 2139
E-mail: gesine.szurman@googlemail.com

Reticular pseudodrusen characterization by retromode imaging

Mariacristina Parravano,¹ Lea Querques,^{1,2} Antonluca Boninfante,¹

Paola Giorno,¹ Monica Varano,¹ Francesco Bandello² and Giuseppe Querques²

¹Fondazione G.B. Bietti-IRCCS, Rome, Italy; ²Department of Ophthalmology, IRCCS San Raffaele Scientific Institute, University Vita-Salute San Raffaele, Milan, Italy

doi: 10.1111/aos.12948

Editor,

Reticular pseudodrusen (RPD) was originally identified as a particular drusen phenotype frequently associated with age-related macular degeneration (AMD), well visible in blue light. New development in retinal imaging methods, such as confocal scanning laser ophthalmoscopy (cSLO), spectral-domain optical coherence tomography (SD-OCT) and adaptive optics, has improved the visualization of RPD. In contrast to conventional drusen, RPD proved to be located internal to the retinal pigmented epithelium (RPE) (Schmitz-Valckenberg et al. 2010; Zweifel et al. 2010; Querques et al. 2012a,b).

Zweifel et al. (2010) and Querques et al. (2012a,b) identified different RPD stages on SD-OCT based on the degree of accumulation of extracellular material. Suzuki et al. (2014) classified RPD on the basis of their appearance in colour fundus photographs and cSLO infrared reflectance (IR) in dot, with a particular target pattern, ribbon and peripheral pseudodrusen.

In this study, we investigated the RPD characteristics on the so-called retromode imaging, which rely on the detection of scattered light from the fundus, and classified RPD on the basis of the appearance of the deposits in the outer retina (i.e. their shape on pseudo-three-dimensional images).

Early AMD patients with RPD (as detected by IR cSLO and SD-OCT) in at least one eye, but without typical drusen, underwent a complete ophthalmic examination, which included retromode imaging of the fundus with the Nidek F-10 (Nidek, Gamagori, Aichi, Japan). The Nidek F-10 is a commercially available cSLO that uses multiple imaging modes including IR, fundus autofluorescence, fluorescein angiography, indocyanine green angiography and retromode. The retromode is a non-invasive imaging

technique that allows us to obtain clear and pseudo-three-dimensional images of the deeper retinal layers by illuminating the fundus with an infrared laser (790 nm) and collecting the scattered light reflected from the retina, choroid and sclera through a semicircular and pericentral aperture by a confocal technique. In detail, while the standard confocal infrared imaging system uses a central aperture, retromode uses aperture on the right side, on the left side and ring aperture. This study was approved by the institutional review board of Fondazione G.B.Bietti-IRCCS.

Nine eyes of seven consecutive patients (five females/two males; mean age 72.1 ± 4.1 years) with RPD and without other AMD-related changes were included. Five fellow eyes were excluded because they were affected with late AMD (geographic atrophy or choroidal neovascularization). In all eyes, RPD was identified by means of laterally scattered light of retromode imaging; this is because the scattered light passing through the laterally oriented aperture created shadows and allowed deeper retinal structures (i.e. RPD) to be visualized. In particular, when the right aperture was used, the dark shadows were in the right side, and RPD deposits appeared as convex structures, which we classified as round, bended and interlacing, detected in variable proportions in all eyes (Fig. 1 A–C).

It has been reported (Acton et al. 2011; Diniz et al. 2013) that retromode imaging of retinal drusen, with lateral confocal aperture, is a highly sensitive technique for detecting and quantifying retinal drusen and was able to detect more deposits than colour fundus photography. Here, we demonstrated the ability of retromode imaging to detect the presence of RPD in all study eyes and to define their shape by producing pseudo-three-dimensional images.

Our study corroborates SD-OCT demonstration that in RPD, the deposits accumulate in the outer retina (rather than in the sub-RPE space as typical drusen do). Moreover, the variable size and different shapes of these deposits (round, bended and interlacing) here described by retromode imaging suggest either the potential existence of different types of pseudodrusen, conferring variable risk for late AMD, or varying progression stages of RPD deposits (Suzuki et al. 2014). The latter hypothesis agrees with previous

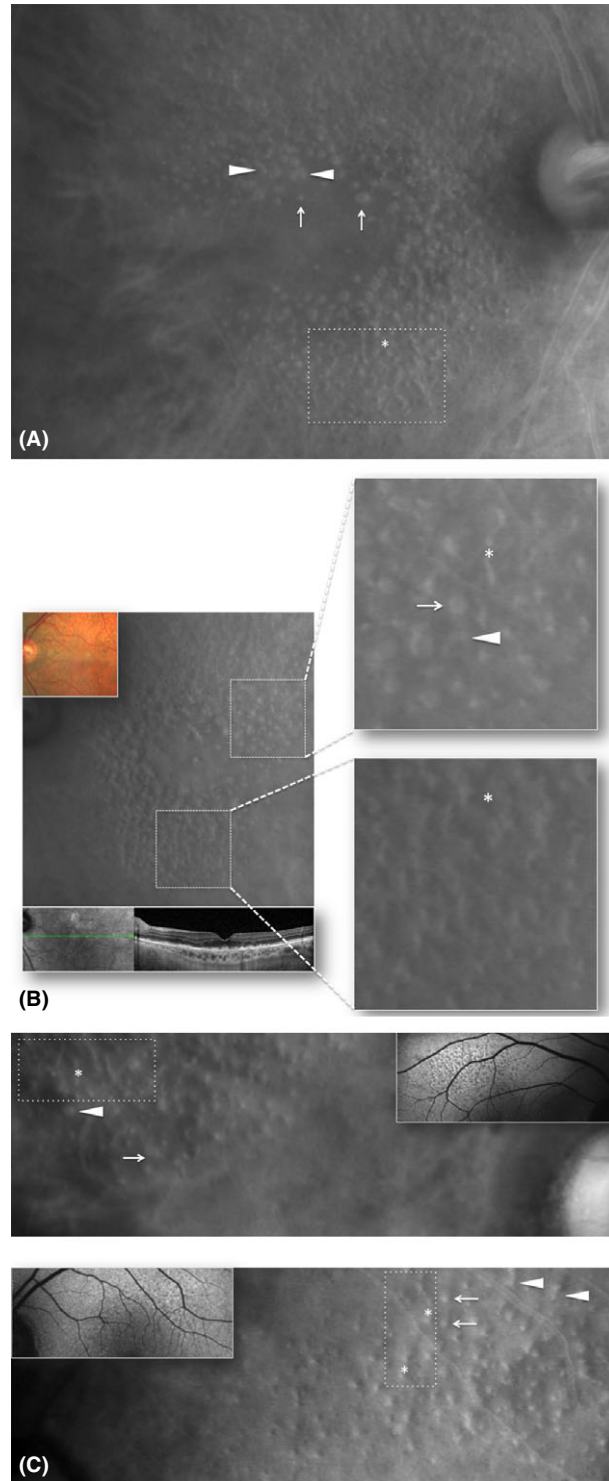


Fig. 1. (A) Retromode imaging of the right eye of patient #3 with reticular pseudodrusen (RPD). On retromode imaging, when the right aperture is used, the dark shadows is in the right side, and RPD deposits appear as variably sized round (arrows), bended (arrowheads) or interlacing (dotted rectangle, asterisk) convex structures. (B) Retromode imaging, colour fundus and spectral-domain optical coherence tomography of the left eye of patient #6 with RPD. Retromode imaging (right aperture with dark shadows in the right side, left panel) shows RPD deposits as variably sized round (enlarged view, upper right panel, arrow), bended (enlarged view, upper right panel, arrowhead) or interlacing (enlarged view, upper and lower right panels, asterisks) convex structures. (C) Retromode imaging and fundus autofluorescence of the right eye of patient #4 and of the left eye of patient #5 with RPD. On retromode imaging (right aperture with dark shadows in the right side) RPD deposits appear as variably sized round (upper and lower panels, arrows), bended (upper and lower panels, arrowheads) or interlacing (upper and lower panels, dotted rectangle, asterisk) convex structures.

reports identifying different SD-OCT stages of RPD, based on the degree of accumulation of extracellular material. Finally, the coexistence in all eyes of different shapes for these deposits, including bended and interlacing, may explain at least in part the reticular appearance previously claimed by different authors as an exclusive peculiarity of the choroid (Querques et al. 2012a,b). Further studies are needed to define the specificity of the retro-mode imaging for detecting RPD.

References

- Acton JH, Cubbidge RP, King H, Galsworthy P & Gibson JM (2011): Drusen detection in retro-mode imaging by a scanning laser ophthalmoscope. *Acta Ophthalmol* **89**: e404–e411.
- iniz B, Ribeiro RM, Rodger DC, Maia M & Sadda S (2013): Drusen detection by confocal aperture-modulated infrared scanning laser ophthalmoscopy. *Br J Ophthalmol* **97**: 285–290.
- Querques G, Canouï-Poitaine F, Coscas F, Massamba N, Querques L, Mimoun G, Bandello F & Souied EH (2012a): Analysis of progression of reticular pseudodrusen by spectral domain-optical coherence tomography. *Invest Ophthalmol Vis Sci* **53**: 1264–1270.
- Querques G, Querques L, Forte R, Massamba N, Coscas F & Souied EH (2012b): Choroidal changes associated with reticular pseudodrusen. *Invest Ophthalmol Vis Sci* **53**: 1258–1263.
- Schmitz-Valckenberg S, Steinberg JS, Fleckenstein M, Visvalingam S, Brinkmann CK & Holz FG (2010): Combined confocal scanning laser ophthalmoscopy and spectral-domain optical coherence tomography imaging of reticular drusen associated with age-related macular degeneration. *Ophthalmology* **117**: 1169–1176.
- Suzuki M, Sato T & Spaide RF (2014): Pseudodrusen subtypes as delineated by multimodal imaging of the fundus. *Am J Ophthalmol* **157**: 1005–1012.
- Zweifel SA, Spaide RF, Curcio CA, Malek G & Imamura Y (2010): Reticular pseudodrusen are subretinal drusenoid deposits. *Ophthalmology* **117**: 303–312.e1.

Correspondence:

Giuseppe Querques
Department of Ophthalmology
IRCCS San Raffaele Scientific Institute
University Vita-Salute San Raffaele
Via Olgettina 60
20132, Milan
Italy
Tel.: +390226432648

Fax: +390226433643
E-mail: giuseppe.querques@hotmail.it

Dr. Parravano and Dr. Varano report personal fees from Allergan, Bayer and Novartis, outside the submitted work; Dr. L. Querques, Dr. Boninfante and Dr. Giorno have nothing to disclose; Dr. Bandello reports personal fees from Alimera, Allergan, Bayer, Novartis, Thrombogenics and Thea, outside the submitted work; and Dr. Querques reports personal fees from Alimera, Allergan, Bayer and Novartis, outside the submitted work. Conception or study design: MP, LQ, GQ. Acquisition, analysis or interpretation of data: MP, GQ, AB, PG. Drafting the manuscript: MP, LQ, GQ. Critical revision of the manuscript: MP, LQ, GQ, MV, FB. Supervision: MP, GQ, MV, FB. The research for this paper was financially supported by Italian Ministry of Health and Fondazione Roma.

Detection of Kayser–Fleischer ring using Scheimpflug imaging

Niklas Telinius,¹ Peter Ott² and Jesper Hjortdal¹

¹Department of Ophthalmology, Aarhus University Hospital, Aarhus, Denmark;

²Department of Hepatology and Gastroenterology, Aarhus University Hospital, Aarhus, Denmark

doi: 10.1111/aos.13271

Editor,

In Wilson's disease (WD), a mutation in ATP7B causes defect in cellular copper transport. As a result, copper accumulates in different tissues, including Descemet's membrane of the cornea, which can be seen in the eye as a Kayser–Fleischer ring (KFR). The KFR can be used to diagnose and monitor the disease (Rodman et al. 1997; Roberts & Schilsky 2008) because it will disappear with successful treatment and reappear with treatment failure. The gold standard for detecting and assessing KFR is slit-lamp examination. Even for the general ophthalmologist, it may be difficult to verify or refuse the presence of a KFR, and a reasonable diagnostic accuracy can only be obtained by ophthalmologists at centres with a suitable number of patients with Wilson's disease. Unless the KFR is prominent, taking photographs of it for clinical records and comparison can be difficult. The aim with this study was to

test whether Scheimpflug imaging can be used for visualizing KFR and thus provide a way to document and quantify KFR. From 2013, all patients with Wilson's disease examined at the ophthalmology department underwent anterior segment Scheimpflug imaging (Pentacam, Oculus) in addition to slit-lamp examination. Slit-lamp examination was conducted by one of two cornea specialists. Scheimpflug images of the inferior part of cornea were analysed in ImageJ by plotting the cross-sectional signal profile. Data are presented as mean \pm SD and analysed using one-way ANOVA with Bonferroni posttest. A total of 21 patients (11 males, 10 females; mean age 33 years, range 14–72) and nine controls were included. These 21 patients comprise 55% of known Danish patients with WD. On Scheimpflug images, the KFR could be seen as a bright subendothelial band peripherally (Fig. 1A). Patients with a KFR ($n = 11$) had a significantly higher subendothelial signal (Fig. 1B) compared to both WD patients without a KFR and the control group, 188 ± 85 versus 81 ± 36 and 106 ± 43 ($p < 0.05$). A KFR could in some cases be visually misdiagnosed due to a different level of brightness of the images. We therefore normalized the subendothelial signal to the epithelial signal (Fig. 1C). Nine out of 11 patients with a KFR had a normalized signal >1 ; the two patients with a ratio <1 had a faint KFR on slit-lamp examination. All controls and 9 of 10 patients without a KFR showed a ratio <1 , except one patient who, however, had a prominent KFR superiorly. The mean for the groups was 1.24 ± 0.39 , 0.62 ± 0.22 and 0.66 ± 0.17 with significant difference between the patients with KFR compared to both other groups ($p < 0.05$). No significant differences were found between patients without a KFR and controls in either absolute subendothelial signal or normalized signal. Ophthalmic imaging modalities have previously been used to describe retinal (Albrecht et al. 2012) and lenticular (Obara et al. 1995) changes in Wilson's disease. This is the first study to our knowledge that reports on ophthalmic imaging of cornea in Wilson's disease. In this brief report, we demonstrate how Scheimpflug imaging can be successfully used to visualize and document the presence of KFR. Scheimpflug does not seem to be more sensitive in detecting KFRs than an experienced ophthalmologist because two patients with faint rings did not differ from controls. The specificity of